

A “Sample-and-Hold” Pulse-Counting Integrator as a Mechanism for Graded Memory Underlying Sensorimotor Adaptation

Jörg Oestreich,^{1,2,*} Nikolai C. Dembrow,¹
Andrew A. George,¹ and Harold H. Zakon¹

¹Section of Neurobiology
The University of Texas at Austin
1 University Station C0920
Austin, Texas 78712

Summary

The mechanisms behind the induction of cellular correlates of memory by sensory input and their contribution to meaningful behavioral changes are largely unknown. We previously reported a graded memory in the form of sensorimotor adaptation in the electromotor output of electric fish. Here we show that the mechanism for this adaptation is a synaptically induced long-lasting shift in intrinsic neuronal excitability. This mechanism rapidly integrates hundreds of spikes in a second, or gradually integrates the same number of spikes delivered over tens of minutes. Thus, this mechanism appears immune to frequency-dependent fluctuations in input and operates as a simple pulse counter over a wide range of time scales, enabling it to transduce graded sensory information into a graded memory and a corresponding change in the behavioral output. This adaptation is based on an NMDA receptor-mediated change in intrinsic excitability of the postsynaptic neurons involving the Ca²⁺-dependent activation of TRP channels.

Introduction

Cellular mechanisms underlying memory formation in the brain are widely studied. However, little is known about how the dynamics of such mechanisms influences the laying down of a neuronal memory, nor has such a mechanism been demonstrated to be critical for any actual behavioral changes.

Sensorimotor adaptation is the appropriate adjustment of a motor output to a persistent change in sensory inflow. It requires the finely graded integration of an error signal. An example is the adaptation to visual distortions induced by prism goggles (Held and Freedman, 1963). We have described a form of sensorimotor adaptation to persistent sensory input in the electromotor system of a weakly electric fish (Oestreich and Zakon, 2002). The wave-type weakly electric brown ghost knife fish (*Apteronotus leptorhynchus*) actively produces an electric field around its body with an electric organ in its tail. The electric organ discharge (EOD) frequency is set by a medullary pacemaker nucleus (PMn). The PMn comprises ~100 pacemaker neurons, which are intrinsic to the nucleus; ~25 relay neurons (Dye and Heiligenberg, 1987), whose axons leave the nucleus and project to spi-

nal electromotoneurons; and small interneuron-like parvocells, whose functions are unknown (Smith et al., 2000). Pacemaker and relay neurons are endogenously active, extensively electrotonically coupled, and set the EOD frequency: for each PMn discharge, the electric organ responds with one EOD (Heiligenberg, 1991). Thus, the behavioral output of the electromotor system directly reflects the electrical activity of its command nucleus. A sine wave of a similar frequency emanating from a nearby fish or generated electronically will jam a fish's electrosensory system. As a consequence, a fish will transiently raise its own EOD frequency to a new value to escape the jamming stimulus; this is the jamming avoidance response (JAR). The JAR is generated by the recruitment of normally quiescent, descending inputs from the sublemniscal prepacemaker nucleus (SPPn) that activates NMDA receptors on relay neurons (Heiligenberg et al., 1996).

We have observed that exposure to a sine wave signal, mimicking the jamming signal from another fish for tens of minutes to hours, results in a long-term resetting of the EOD frequency to a new frequency that is less likely to be jammed (Figure 1A). This is an ecologically relevant situation for this species, as individuals may be in close proximity with each other for tens of minutes or longer when they are in hiding during the daytime (Oestreich and Zakon, 2005). Under these conditions, fish perform a JAR followed by LTFE (J.O., unpublished data). The EOD frequency may remain elevated for hours following termination of the jamming stimulus. This sensorimotor adaptation, termed long-term frequency elevation (LTFE), is a form of nonassociative memory.

The magnitude of the adaptation in vivo is graded with respect to stimulus amplitude and duration (Oestreich and Zakon, 2002). Neural correlates for LTFE exist in a slice preparation of the PMn (Figures 1B and 1C) (Dye, 1988; Oestreich and Zakon, 2002), allowing us to directly relate changes in neuronal activity to changes in behavior. Here we show that this behaviorally relevant form of neural adaptation functions as a “sample-and-hold” pulse counter. We show that the adaptation is produced by a broad but potentially behaviorally relevant range of afferent firing frequencies and patterns consistent with the idea that the mechanism integrates synaptic input by counting pulses. We demonstrate that the adaptation is due to a change in intrinsic excitability of the postsynaptic neurons, rather than continued synaptic input, and that it is dependent on an NMDA receptor-mediated influx of Ca²⁺ and activation of TRP cationic channels.

Results

The Dynamic Range of the Behavior in the Whole Fish Is Set by the Pacemaker Nucleus

We compared the dynamic range of JAR and LTFE in the behaving animal with fictive JAR and LTFE in the PMn slice. We tested the maximum range of the JAR by driving the fish with a strong stimulus amplitude (100 mV/cm) that was constantly adjusted to follow

*Correspondence: joerg_oestreich@hms.harvard.edu

²Present address: Harvard Medical School, Department of Neurobiology, 220 Longwood Avenue, Boston, Massachusetts 02115.

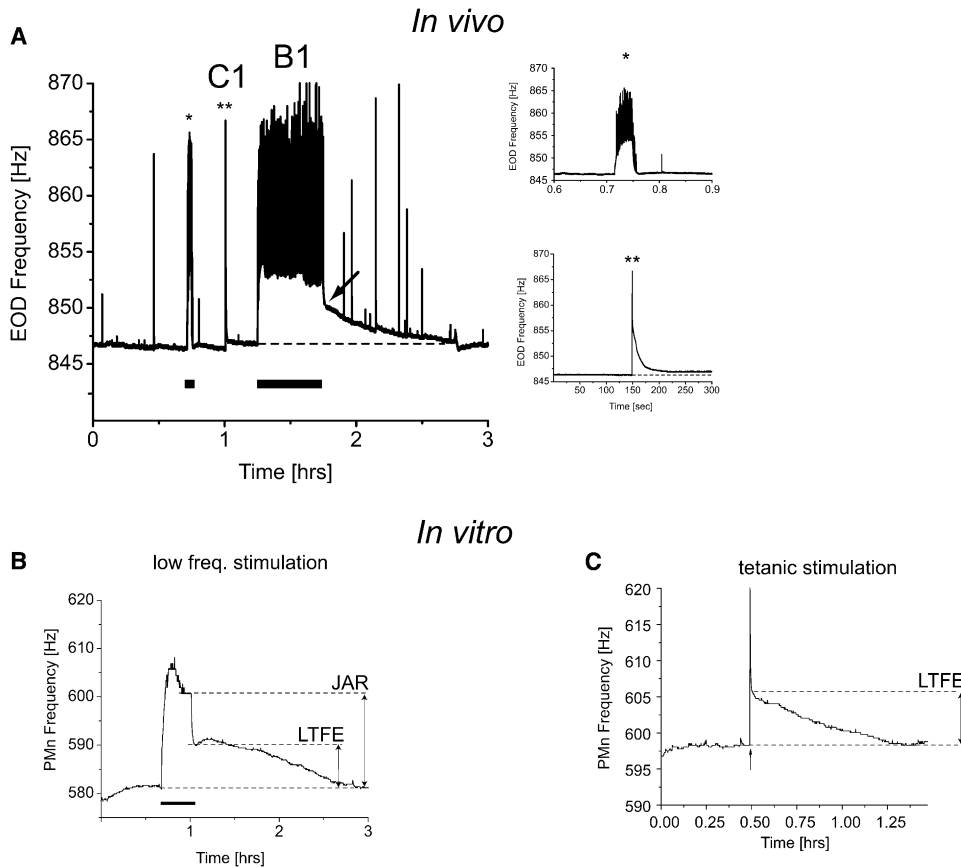


Figure 1. Behavioral EOD Frequency Modulations in *Aptereronotus leptorhynchus* and Their Neural Correlates

(A) EOD frequency in response to stimulation with an artificial sine wave mimicking the presence of a conspecific in jamming frequency range ($\Delta F = -3$ Hz; stimulus periods marked by black bar underneath EOD frequency trace). An initial short stimulus presentation of 2 min leads to a JAR (*, see inset), after which the EOD frequency returns back to baseline. This depicts the usual stimulus paradigm, historically used to describe the JAR (Bullock et al., 1972; Dulka and Maler, 1994; Dye, 1987; Heiligenberg et al., 1996). In contrast, a stimulus presentation of 30 min leads to a prolonged JAR, which is followed by a lasting EOD frequency elevation (arrow) beyond the duration of the stimulus signal (LTFE, long-term frequency elevation), which only gradually returns to baseline. LTFE can also be seen after yodels or rises (**, see inset), a spontaneous, EOD frequency modulation of rapid onset (Dye, 1987) and with varying communicatory function (Tallarovic and Zakon, 2002). Rapid EOD frequency deflections (in [A]) outside of the stimulus period are other yodels, whereas fast increases during the stimulus periods on top of the JAR are chirps, a third type of communication signal. Chirps are an aggressive signal predominantly produced by males (Dulka and Maler, 1994; Hagedorn and Heiligenberg, 1985). They are controlled by a different pathway originating from a second prepacemaker nucleus, which is not a subject of this study (Dye et al., 1989; Heiligenberg et al., 1996; Juranek and Metzner, 1998). The letters B1 and C1 refer to the neural correlates for JAR and yodels in vitro, shown in (B) and (C), respectively. (B) A neural correlate for the JAR and LTFE exists in vitro in the PMn brain slice preparation: prolonged low-frequency stimulation over 20 min of the terminal portion of the afferent fiber bundles arising in the prepacemaker nuclei produces a fictive JAR in the PMn frequency, which is followed by LTFE. (C) A 1 s long tetanic burst stimulation of the afferent fibers produces the neural correlate of a yodel, which is followed by lasting LTFE.

3 Hz below the fish's EOD frequency. Under these conditions, the JAR saturated at 24.3 ± 1.2 Hz ($n = 32$; Figure 2A). Because the fish did not maintain such a large JAR for more than a few minutes and because LTFE magnitude in vivo is dependent on stimulus duration (Oestreich and Zakon, 2002), only little LTFE was induced. In contrast, using the same stimulus signal amplitude at a static frequency of 3 Hz below the fish's EOD frequency just prior to stimulus presentation resulted in a stable JAR of lower magnitude (10.5 ± 1.2 Hz; $n = 5$), which is followed by a large amount of LTFE of 9.5 ± 1.3 Hz ($n = 6$) (Oestreich and Zakon, 2002) (Figure 2B).

We then tested the dynamic range of the fictive JAR and LTFE in vitro by increasing stimulus intensities used to drive the afferent fibers to the PMn until the eli-

cited PMn frequency increase was saturated. For each of the stimulus amplitudes, a different group of PMns was used to avoid progressive buildup of LTFE with increasing stimulus amplitudes in individual preparations. Fictive JAR and LTFE both exhibit a sharp threshold and are positively correlated with the stimulus magnitude until saturation is reached at 24.6 ± 4.8 Hz ($n = 7$) for the fictive JAR and 12.2 ± 3.2 Hz ($n = 7$) for LTFE (Figure 2C). These values correspond closely to the behavioral values (in red), suggesting that the dynamic range of the animal's behavior is completely predicted by the properties of the PMn neurons. Furthermore, these results allow us to choose a stimulus level (100 nA) in some experiments that will recruit all the afferents and therefore minimize variation in the numbers of afferents recruited across different preparations.

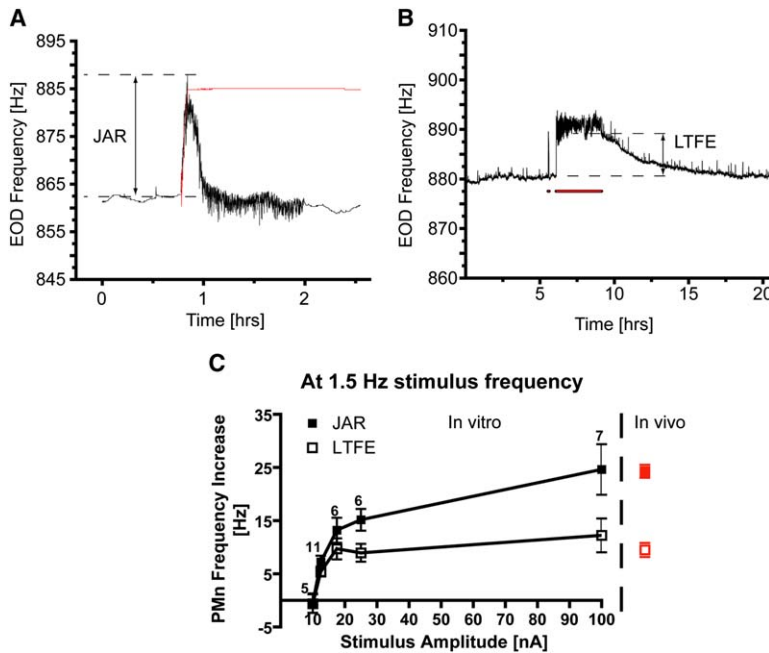


Figure 2. The Dynamic Range of JAR and LTFE In Vivo and In Vitro

(A) JAR in a fish stimulated with a dynamic stimulus signal. The stimulus frequency (in red) was adjusted by a computer, so that it would follow the fish's EOD frequency (in black) with a constant difference of -3 Hz (100 mV/cm) in the upward direction. These conditions resulted in a large JAR magnitude, which was only maintained for a few minutes, before the fish's EOD frequency usually returned back to baseline frequency. These stimulus conditions did not result in LTFE (defined as the stable frequency elevation from baseline after the initial rapid drop following stimulus offset in [B]). The average maximum JAR magnitude under these stimulus conditions (red JAR value in [C] = red filled square) corresponds to the maximum magnitude of the fictive JAR in vitro. (B) JAR and LTFE in a fish stimulated with a static stimulus frequency (in red), 3 Hz (100 mV/cm) below the fish's EOD frequency (in black). Under these conditions, the fish maintains a JAR of lower magnitude even for 3 hr, which induces LTFE. Such stimulation saturates LTFE (Oestreich and Zakon, 2002). (C) Average fictive JAR and LTFE magnitudes in different groups of PMNs in response to increasing stimulus

amplitudes in vitro. In these experiments, the afferent fiber pathways to the PMn were stimulated with increasing stimulus amplitudes for 20 min at 1.5 Hz using triple pulses. Note the sharp threshold at 10 nA for activating the PMn frequency change: increasing the stimulus amplitude by 2.5 nA already results in a mean fictive JAR magnitude, which is 29.4% of the maximum magnitude at 100 nA, and LTFE, which is 44.1% of the saturated magnitude. LTFE is virtually saturated by 17.5 nA. The saturated values at 100 nA closely correspond to the in vivo values for JAR and LTFE (red filled or empty square, respectively). In vivo data for LTFE in (B) and (C) are from (Oestreich and Zakon, 2002).

The LTFE Mechanism Integrates Stimulus Pulses Over a Wide, Linear Range

Besides being graded with stimulus amplitude, LTFE amplitude both in vivo and in vitro also depends on stimulus duration (Oestreich and Zakon, 2002). Specifically, in vitro, two min long stimulations produce significantly less LTFE than 20 min long stimulations. Using a range of stimulus durations to estimate whether LTFE could accumulate after a small number of stimulus pulses, we examined how many pulses could be integrated and whether that integration was linear (Figures 3A and 3B). A significant amount of LTFE (1.7 ± 0.5 Hz compared to -0.02 ± 0.05 Hz of baseline change in controls over a similar time period; $p < 0.0001$, t test) accumulated after our briefest stimulus (7.5 s, 1.5 Hz, triple pulses), which produced a total number of only 33 pulses (Figure 3C). With longer stimulus durations in different groups, LTFE increased gradually and linearly until it reached a maximum level of 12.2 ± 3.2 Hz by 20 min of stimulation ($p < 0.0001$; ANOVA, followed by post test for linear trend) (Figure 3A). Thus, LTFE is evident after a small number of stimuli (33) and develops rapidly (7.5 s) but can continue to increment linearly over many stimuli (5400 pulses at 20 min) until it saturates around 20 min of stimulation. The LTFE mechanism thus seems to integrate synaptic input over a wide dynamic range.

The LTFE Mechanism Behaves as a Pulse Counter

If an integrator is to be linear and operate over a wide range of frequencies, it must be insensitive to variations in spike patterns. We tested this at nonsaturating stimulus levels (12.5 nA) by presenting the PMn with a con-

stant numbers of pulses but at different stimulus rates and durations (1.5 Hz for 20 min, 3.0 Hz for 10 min, 6.0 Hz for 5 min). We observed a significant difference in the magnitude of the fictive JARs (ANOVA, $p < 0.05$) but no differences between groups using various post hoc analyses corrected for multiple comparisons (e.g., Bonferroni test). There were no significant differences in the magnitude of LTFE over this frequency range in either overall tests of significance or comparisons of group means (Figures 4A and 4B).

We then tested whether the magnitude of LTFE was sensitive to stimulus patterns that produced different instantaneous rates of input. PMNs were either stimulated with triple pulses per bout (spaced 25 ms apart) at 1.5 Hz, or with a single pulse per bout at 4.5 Hz. In this way, the overall number of pulses was kept constant despite large differences in the instantaneous firing rate. To prevent LTFE saturation from occurring, PMNs were only stimulated for 2 min. No difference was found in fictive JAR and LTFE magnitudes between these groups despite the difference in instantaneous frequency (4.5 Hz in the single-pulse group, 40 Hz in the triple-pulse group; fictive JAR and LTFE: $p > 0.05$, t test; Figures 4C and 4D). Thus, the LTFE mechanism integrates synaptic stimulus pulses without consideration of the pattern of input or their instantaneous firing frequency, but functions as a pulse counter.

Tetanic Induction of LTFE

Apteronotus make a spontaneous rapid modulation of the EOD frequency of varying communicatory function called a yodel or rise (Dye, 1987; Tallarovic and Zakon, 2002) (Figure 1A, double asterisks). It is believed that

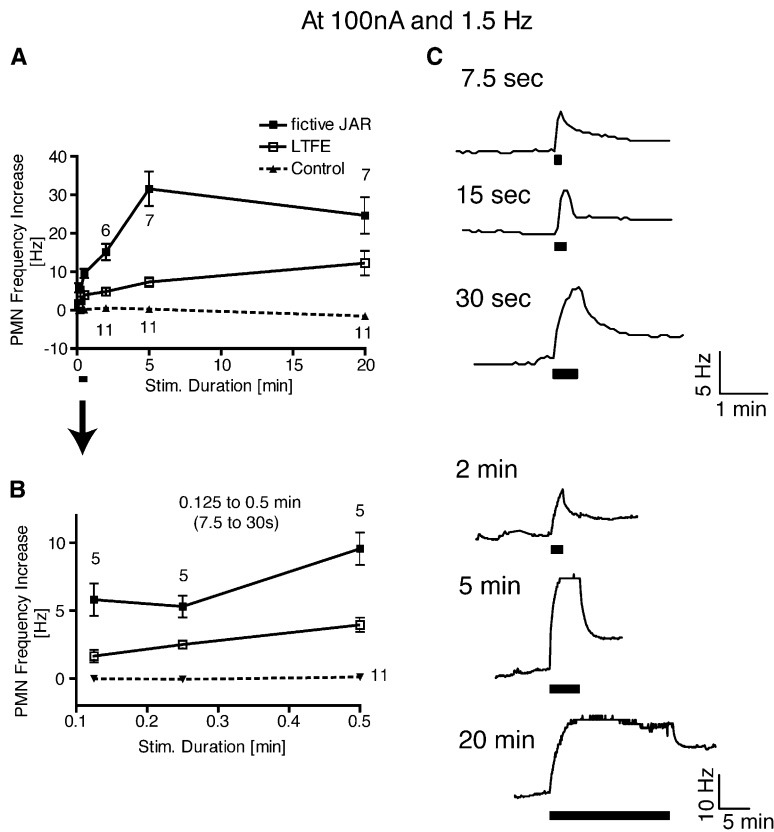


Figure 3. LTFE Develops Over Tens of Minutes

Different groups of PMn were stimulated at 1.5 Hz and 100 nA for increasing durations. The numbers of experiments per group are reported above the values. Frequency changes in the stimulated groups are compared to baseline changes at corresponding time points in an unstimulated control group ($n = 11$). (A) LTFE (open squares) is significantly different from baseline changes after 7.5 s (B) and increases gradually with longer stimulus durations. The fictive JAR (filled squares) increases nonproportionally in comparison to LTFE and reaches a maximum by 5 min. (B) Magnification of the first 30 s in (A). (C) Example traces for groups stimulated with increasing durations. The black bar indicates the stimulus period.

yodels result from a high-frequency barrage of input to the PMn that activates NMDA receptors (Dye, 1988; Dye et al., 1989; Dye and Heiligenberg, 1987); thus, the response of the PMn to in vitro tetanic stimulation is a likely neural correlate of yodeling. LTFE can also be activated in vitro by tetanic stimulation of the afferent fibers leading to the PMn (Dye, 1988). Despite an initial report that LTFE following tetanic stimulation of the PMn slice lasted only for tens of seconds, we observe LTFE after a single tetanic burst for tens of minutes in vitro (Figure 1C). Similarly, LTFE can also be observed after yodels in vivo (Figure 1A, double asterisks, inset).

Does LTFE elicited by low rates of stimulation over many minutes and LTFE induced within 1 s by a tetanic burst share the same mechanism, or are separate intracellular signaling pathways activated? LTFE induced by tetanic stimulation is abolished by the NMDA receptor antagonist d-APV (Dye et al., 1989). We tested whether NMDA receptor activation is also responsible for mediating low-frequency-induced LTFE. We found that $\sim 350\text{--}500 \mu\text{M}$ of the NMDA receptor antagonist CPP effectively blocked the fictive JAR and LTFE (JAR: $p < 0.01$, LTFE: $p < 0.05$, ANOVA followed by Dunnett's post hoc test; Figures 5A and 5B). We then tested whether a series of tetanic stimuli would saturate the LTFE mechanism and occlude the development of further LTFE by prolonged low-frequency stimulation. PMns were initially stimulated with three tetanic bursts of 1000 Hz and 1 s duration each, spaced 2 min apart to ensure that LTFE was saturated. Each stimulation resulted in a maintained step up in spike frequency with the magnitude of the increase becoming progressively

smaller, suggesting saturation of a component in the LTFE pathway (Figure 5C).

Twenty minutes later, low-frequency stimulation at 1.5 Hz resulted in a fictive JAR of normal magnitude ($p > 0.05$, t test; Figure 5E) but reduced LTFE when compared to a control group of PMns, which were not tetanically stimulated prior to the low-frequency stimulation ($p < 0.05$, t test; Figure 5F). The sum of LTFE after tetanic and low-frequency stimulation was equal to LTFE in the control group (Figure 5F; $p > 0.93$, t test). Within the group that received the tetanic stimulation, LTFE after the low-frequency stimulation was inversely correlated (fitted with a one-phase exponential decay, $r^2 > 0.81$; Figure 5G). These data show that LTFE induced by high-frequency stimulation occludes LTFE following low-frequency stimulation and suggest that both stimulus paradigms converge onto the same mechanism for LTFE.

If the LTFE mechanism is truly counting pulses, then the same amount of LTFE should accrue whether the stimulus is tetanic or gradual. The magnitude of LTFE caused by the first tetanic stimulation of 1000 pulses was 5.6 ± 0.4 Hz. In comparison, after 5 min of low-frequency stimulation as in the previous experiment, during which 1350 pulses were delivered, LTFE magnitude was 7.3 ± 1.3 Hz. Correcting for the difference in the number of pulses given by the two stimuli and assuming linearity, we calculate that after 1000 pulses the magnitude of LTFE to the slow stimulation would be 5.47 Hz. Again, this result suggests that under extremely different conditions of stimulation (1000 Hz

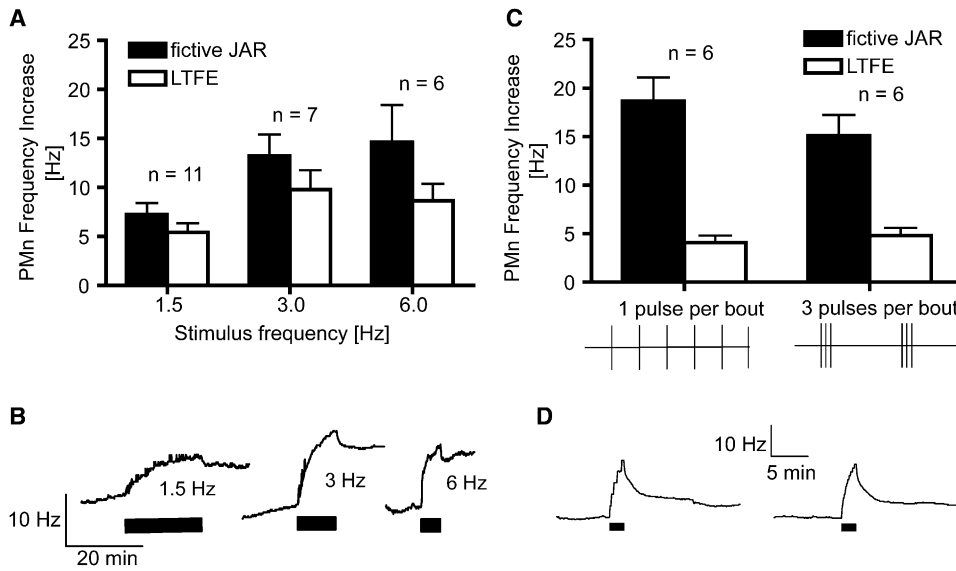


Figure 4. The LTFE Mechanism Behaves as a Pulse Counter

(A) Presentation of different groups of PMns with a constant number of pulses but different stimulus rates and durations under nonsaturating conditions at 12.5 nA stimulus amplitude. Stimulus pulses were delivered at 1.5 Hz for 20 min, 3.0 Hz for 10 min, and 6.0 Hz for 5 min. Each bout was comprised of three pulses, separated by 25 ms. No significant difference in fictive JAR and LTFE magnitude between different groups was observed ($p > 0.05$, all cases). (B) Example traces for the experiment described in (A). (C) Insensitivity of LTFE to variations in stimulus patterns with different instantaneous pulse rates. Group 1 was stimulated with the same number of stimulus pulses, but with only one pulse per bout, delivered at 4.5 Hz. Group 2 was stimulated with triple pulses per bout, separated by 25 ms, and delivered at 1.5 Hz. The stimulus amplitude was 100 nA, and stimulus duration 2 min, where LTFE is not saturated yet. This allowed for possible increases or decreases in LTFE magnitude. No significant difference between fictive JAR and LTFE was observed ($p > 0.05$, both cases). (D) Example traces for the experiment described in (C).

versus 1.5 Hz) LTFE acts as a pulse counter and disregards temporal information in input spike trains.

LTFE Is Induced, but Not Maintained, by Synaptic Stimulation

We presume that LTFE is maintained by changes in intrinsic conductance of neurons in the PMn. It is possible, however, that the maintenance phase of LTFE might be due to alterations in synaptic input, such as tonic transmitter release from synaptic terminals. N-type Ca^{2+} channels are often found in the synaptic terminal, where they mediate Ca^{2+} influx and subsequent release of synaptic vesicles (Meir et al., 1999). Application of the N-type Ca^{2+} channel blocker ω -conotoxin GVIA 20 min before the stimulation of the slice had no effect on the baseline firing frequency, but effectively blocked the fictive JAR and LTFE (mean of p values: $p = 0.002$, compared to saline controls during stimulation, and $p = 0.003$, after stimulation; Figure 6). These results suggest that N-type Ca^{2+} channels exclusively mediate the conductance of Ca^{2+} into the presynaptic terminal of the prepacemaker afferents and, as reported previously, N-type Ca^{2+} channels are not involved in generating the basic PMn firing rate (Smith and Zakon, 2000). We then tested whether synaptic transmission was involved in the maintenance of LTFE by applying the conotoxin 5 min after the end of the stimulation, once LTFE had already been induced. If synaptic transmission plays a role, conotoxin should lower the PMn frequency elevation back to baseline. In contrast, we found that the conotoxin did not affect the magnitude of LTFE when compared to a saline-treated control group (mean of p values: $p = 0.8$, comparing curve to saline control dur-

ing stimulation, and $p = 0.7$, after stimulation; Figure 6). These data strongly support the hypothesis that LTFE is maintained by changes in intrinsic excitability of the PMn neurons rather than by continuing synaptic activity.

LTFE Depends on Ca^{2+} Influx and TRP Channels

As outlined above, NMDA receptor activation is necessary for stimulus-induced LTFE. Direct application of NMDA to the PMn also produces a long-term frequency elevation (LTFE_{NMDA}) (Dye et al., 1989) (Figure 7A). We examined whether altering the Ca^{2+} influx through NMDA receptors might change LTFE_{NMDA} magnitude (Figure 7A and Table 1). Lowering extracellular Ca^{2+} to nominally free levels reduces the LTFE_{NMDA} magnitude. LTFE_{NMDA} was significantly reduced whether Ca^{2+} was replaced with Mg^{2+} (2x Mg^{2+}) or not (1x Mg^{2+}). Conversely, increasing extracellular Ca^{2+} concentration (3.3 mM) significantly enhanced LTFE_{NMDA} magnitude (3x Ca^{2+}). These data suggest that LTFE is induced by Ca^{2+} influx through NMDA receptors in a dose-dependent manner.

Previously, it has been shown that NMDA-induced elevations in firing frequency are accompanied by depolarization in the PMn neurons (Dye, 1988). Ca^{2+} -activated nonspecific cation currents (CAN) have been described in a number of neuronal systems (see Partridge et al., 1994, for review). CAN currents that do not inactivate or inactivate very slowly are capable of maintaining sustained membrane potential depolarization and thus a prolonged increase in spike frequency. Recent research suggests that transient receptor potential channels (TRP) may be the molecular constituents of CAN currents (Launay et al., 2002; Prawitt et al., 2003).

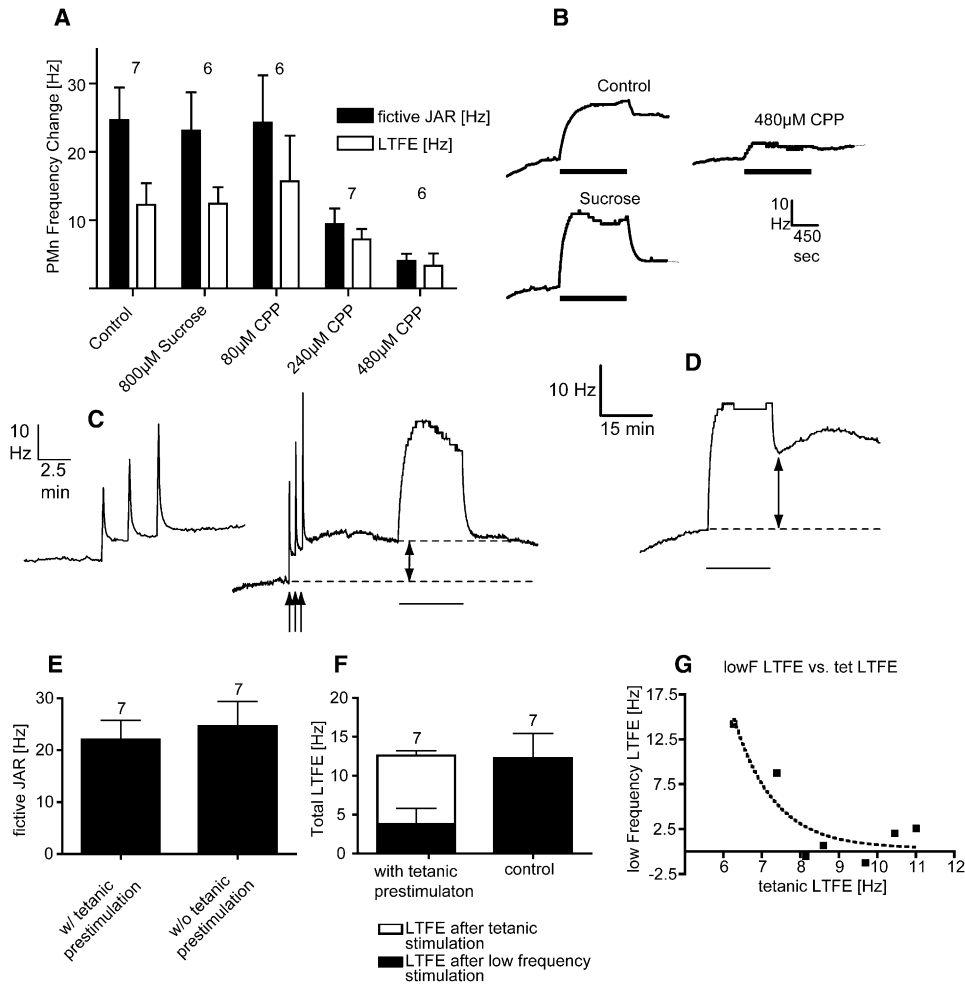


Figure 5. LTFE Activation by Low-Frequency and Tetanic Stimulation Shares a Common NMDA Receptor-Dependent Intracellular Pathway
(A) Effect of NMDA receptor block on low-frequency-induced PMn frequency increase. 480 µM CPP effectively abolished fictive JAR and LTFE at 1.5 Hz, 20 min, and 100 nA (ANOVA with Dunnett's post hoc analysis; fictive JAR: $p < 0.01$, LTFE: $p < 0.05$; fictive JAR and LTFE: 80 µM and 240 µM groups not significantly different from controls at $p > 0.05$). This emphasizes that NMDA receptors are involved in mediating low-frequency-induced LTFE. Control application of 800 µM sucrose to test for possible osmolarity effects did not affect fictive JAR and LTFE when compared to controls (both: $p > 0.05$). Bars represent mean values of different groups of PMn. **(B)** Example traces for a subset of the experiments described in **(A)**. **(C–F)** Low-frequency-induced LTFE is occluded by preceding high-frequency stimulation, suggesting that both stimulus paradigms induce LTFE via the same mechanism. **(C)** Example trace for an experiment with a tetanic prestimulation. The inset shows a magnification of the trace during the initial tetanic stimulation. Three bouts of stimulation at 1000 Hz, for 1 s, and separated by 2 min, where administered, and produced LTFE. 20 min later, low-frequency stimulation at 1.5 Hz for 20 min led to a fictive JAR of normal magnitude, but failed to induce LTFE. Stimulus amplitude in both cases was 100 nA. **(D)** An example trace of a control experiment without tetanic prestimulation shows a fictive JAR, followed by LTFE. **(E)** Tetanic stimulation did not affect the mean magnitude of the fictive JAR when compared to a group without tetanic prestimulation. **(F)** The sum of low- and high-stimulation frequency-induced LTFE was comparable to LTFE in the control group. **(G)** Within each PMn, low-frequency-induced LTFE was inversely correlated with LTFE after the previous tetanic stimulation. This relationship was fitted with a one-phase exponential decay ($r^2 > 0.81$).

We examined whether TRP channels might contribute to the maintenance of LTFE. We found that flufenamic acid (FFA), which has been shown to inhibit TRP channel-mediated currents (Hill et al., 2004; Inoue et al., 2001; Tesfai et al., 2001; Tozzi et al., 2003; Ullrich et al., 2005), reversibly reduced the magnitude of tetanically induced LTFE in a dose-dependent manner (Figure 7B and Table 1). Inhibition by FFA was incomplete (~75% at 100 µM) but nonetheless significant. Other studies have found that 100 µM FFA does not completely inhibit CAN currents and that a more complete block may be achieved with 200–1000 µM FFA (Hill et al., 2004; Inoue et al., 2001; Lee et al., 2003; Tozzi

et al., 2003; Zhu et al., 2005). We found that high concentrations of FFA (>100 µM, $n = 3$, data not shown) uncoupled the normally highly regular field potentials of the pacemaker nucleus, presumably due to FFA's effects upon the gap junctions (Harks et al., 2001; Srinivas and Spray, 2003) that keep the syncytium of neurons firing at the same frequency (Moortgat et al., 2000a, 2000b). To confirm that the effects of FFA were targeting TRP channels and not other possible FFA targets (Eder et al., 1998; Harks et al., 2001; Srinivas and Spray, 2003), we examined the sensitivity of LTFE to two other known TRP blockers: MDL12,330A and SKF96365 (van Rossum et al., 2000; Zhu et al., 1998). Both MDL12,330A

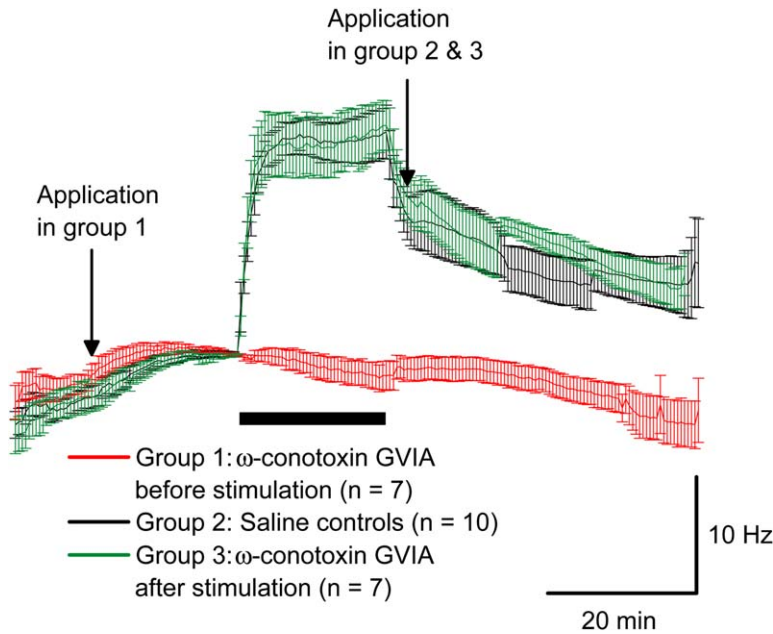


Figure 6. Pharmacological Blockade of Synaptic Input to the PMn Reveals that LTFE Maintenance Is Independent of Further Synaptic Activity

Block of synaptic N-type Ca^{2+} channels by ω -conotoxin GVIA abolishes fictive JAR and LTFE, when applied before the stimulation (mean of p values: $p = 0.002$, comparing curve to a saline-treated control group during stimulation, and $p = 0.003$, after stimulation). If applied after stimulation, the conotoxin does not affect LTFE when compared to the saline-treated control group (mean of p values: $p = 0.8$, comparing curve to saline control during stimulation, and $p = 0.7$, after stimulation), suggesting that synaptic activity does not play a role in maintaining LTFE. Plotted are mean values of the PMn frequency in different PMn collected every 30 s. Curves were not significantly different before stimulation ($p > 0.2$).

and SKF96365 also significantly reduced the frequency elevation following stimulation of the afferent fibers (Table 1).

To confirm that these TRP inhibitors were not simply preventing glutamate release from the pacemaker afferents, we examined their effects on $\text{LTFE}_{\text{NMDA}}$. FFA, MDL12,330A, and SKF96365 all reversibly reduced $\text{LTFE}_{\text{NMDA}}$ (Figure 7C and Table 1). Thus, it appears that Ca^{2+} influx through NMDA receptors activates and/or enhances a TRP channel-mediated current that underlies LTFE.

We then examined whether a TRP channel that is gated by a rise in intracellular Ca^{2+} is found in the PMn. We cloned from *Apteranotus* PMn RNA a candidate TRP subunit gene known to have this property (TRPM5, GenBank accession number: bankit757517) (Hofmann et al., 2003; Prawitt et al., 2003) (Figure 8A). The portion of the gene that we sequenced had an 81% identity and 92% similarity with TRPM5 from the mouse; the pore region had 37 of 38 amino acids identical (97%) with the mouse. We then determined that aptTRPM5 is expressed in the PMn by in situ hybridization. TRPM5 was localized to both pacemaker (~ 25 – $50 \mu\text{m}$) and relay (~ 70 – $100 \mu\text{m}$) neurons (Figures 8B and 8C). As negative controls, hybridizations performed with digoxigenin-labeled sense RNA (Figure 8D) or competition of the labeled antisense probe with excess nonlabeled antisense RNA (Figure 8E) showed no specific labeling of pacemaker or relay neurons.

Discussion

The Pacemaker Nucleus Is the Locus of Adaptation: Linking Neurons to Behavior

It is often difficult to locate in the nervous system the site of a specific behavioral change or, conversely, determine how plasticity in brain slices or dissociated cells relates to behavior. Here we report that sensorimotor adaptation in the electromotor system, which is reflected by LTFE in the EOD frequency, is initiated in a pacemaker

slice by similar parameters of stimulus duration and magnitude that activate adaptation in vivo (Oestreich and Zakon, 2002). Further, we show that the maximum magnitude of adaptation in the PMn in vitro is identical to the maximum magnitude of adaptation in vivo. We also show that while presynaptic input initiates LTFE, it results from changes in excitability that occur exclusively in the postsynaptic neurons of the PMn. From this we conclude that this simple form of adaptation results from changes in the neurons of the PMn. Because we are able to localize this plasticity to a specific nucleus and we understand how these neurons generate behavioral output, we can demonstrate how a specific form of adaptive cellular plasticity contributes to behavior.

The Adaptation Mechanism Is a Sample-and-Hold Pulse Counter

In the isolated PMn in vitro, LTFE shows time/intensity trading. That is, the same magnitude of LTFE can be achieved with a low pulse rate over a long duration or a rapid pulse rate over a short duration. The LTFE integration mechanism is immune to variation in the temporal pattern of inputs over an astonishing ~ 1000 -fold variation in input spike frequency or, to put it another way, whether the pulses occur abruptly in 1 s or gradually over 5 min. The cellular mechanism for LTFE integrates the number of stimulus pulses it receives, accomplishing this rapidly, yet maintaining the last value reached for many tens of minutes. Thus, it behaves as a sample-and-hold pulse counter and endows the system with a broad-band response.

We predict that this may be a general mechanism for sensorimotor or other forms of adaptation where input spike trains must be transduced into long-term changes in postsynaptic excitability in a graded manner.

The Cellular Basis of Sample-and-Hold Pulse Counting

To ensure that the adaptive mechanism is activated in a graded fashion, the integration of synaptic events would

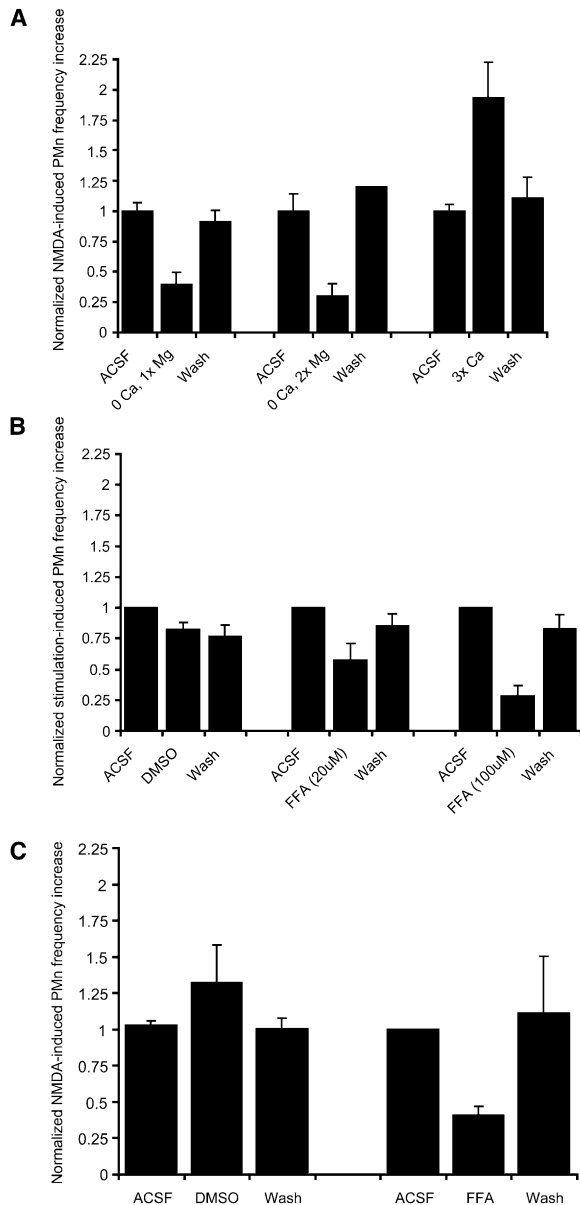


Figure 7. LTFE Is Sensitive to External Ca²⁺ Concentration and TRP Channel Antagonists

(A) The NMDA-induced increase in PMn frequency (LTFE_{NMDA}) is dependent on external Ca²⁺ concentration. If the Ca²⁺ concentration in the ACSF is zero, LTFE_{NMDA} is reduced. This reduction is not due to nonspecific effects of the decrease in surface charge, because replacing Ca²⁺ with Mg²⁺ to keep the surface charge constant does not increase LTFE_{NMDA} back to normal. Increasing the external Ca²⁺ concentration 3-fold enhances LTFE_{NMDA}. (B) The TRP channel blocker flufenamic acid (FFA) reduces stimulus-induced LTFE in a dose-dependent fashion. (C) FFA also reduces LTFE_{NMDA}. In each experiment, baseline LTFE was first determined in normal ACSF by either applying NMDA (A and C) or stimulating the afferent fibers (B). Two hours later, LTFE was tested in different ACSF either containing changed Ca²⁺ concentrations (A), or DMSO, or FFA in DMSO (B and C). After a 2 hr wash in normal ACSF, LTFE was retested again. In all cases, LTFE returned to normal. In (B) and (C), DMSO was applied as a control in a separate group of PMn.

have to be linear as well. The first stage in this process is due to the linear behavior of the NMDA receptor. NMDA receptors are noted for their nonlinearity, but two things

Table 1. Different TRP Channel Inhibitors All Reduce LTFE

Treatment	Mean % of Control ± SE	n	p Value
On stimulus-induced LTFE			
FFA (20 μM)	57.7% ± 13.1%	6	<0.01
FFA (100 μM)	28.7% ± 8%	4	<0.01
MDL 12,330A (10 μM)	45.39% ± 7.9 %	7	<0.01
SKF 96365 (20 μM)	30.8% ± 4.5 %	5	<0.01
On LTFE_{NMDA}			
0 Ca, 2x Mg ²⁺	30% ± 10%	6	<0.001
0 Ca, 1x Mg ²⁺	39.6% ± 9.7%	3	<0.001
3x Ca	193.4% ± 29.1%	6	<0.05
FFA (20 μM)	40.8% ± 6.4%	4	<0.05
MDL 12,330A (10 μM)	42.3% ± 4.9 %	5	<0.05
SKF 96365 (20 μM)	79.9% ± 7.5 %	4	<0.05

TRP channel inhibitors flufenamic acid (FFA), MDL12,330A, and SKF96365 all reduce stimulus-induced LTFE and LTFE_{NMDA}. Mean percentage of control ± SE represents the percentage of control that the experimental condition produced, averaged over the sample size (n). p value represents the significance as determined using an ANOVA, followed by Bonferroni's post hoc analysis.

contribute to their linearity in the pacemaker (Daw et al., 1993). Cloned NR1/NR2B NMDA receptors from *A. leptorhynchus* brain show reduced Mg²⁺ affinity when compared to murine receptors (but exhibit similar characteristics otherwise) (Harvey-Girard and Dunn, 2003). In addition, the high spontaneous firing rate of the PMn neurons would likely keep Mg²⁺ from the pore. Therefore, Ca²⁺ would always flow through NMDA receptors of the neurons in the pacemaker nucleus when glutamate is bound, even during low-frequency afferent stimulation. Thus, the higher the stimulus frequency, the more postsynaptic NMDA receptors will be activated and the more Ca²⁺ will flow into the cell, activating the LTFE mechanism in a graded manner. In support of this idea, we show that the magnitude of LTFE depends on the extracellular Ca²⁺ concentration (Figure 9).

The two major neuronal cell types in the PMn, relay and pacemaker cells, have been shown to express two different splice variants of the NR1 subunit using in situ hybridization (Bottai et al., 1997, 1998). Although an antibody against the NR1 subunit only labeled relay cells (Spiro et al., 1994), the in situ studies are consistent with in vivo electrophysiological and pharmacological studies suggesting that both relay and pacemaker cells receive input via NMDA receptors (Dye et al., 1989; Dye and Heiligenberg, 1987; Heiligenberg et al., 1996). Relay cells receive NMDA-receptor-dependent input from one input pathway (the SPPn), whereas pacemaker cells receive it from another (the thalamic prepacemaker nucleus portion G) (Heiligenberg et al., 1996). We selectively activated the pathway to the relay neurons with the stimulus regime used in our behavior experiments, but behavioral activation of the NMDA receptors on the pacemaker neurons causes a JAR-like response as well (the nonspecific response) (Heiligenberg et al., 1996), and this may also be followed by LTFE (J.O., unpublished data). Because fiber pathways from both input nuclei traverse the tissue rostral of the PMn and cannot be selectively stimulated in the slice, out of necessity we stimulated them both. However, since both pacemaker and relay neurons possess NMDA receptors with NR1, NR2A, -B, and -C subunits (E. Harvey-Girard,

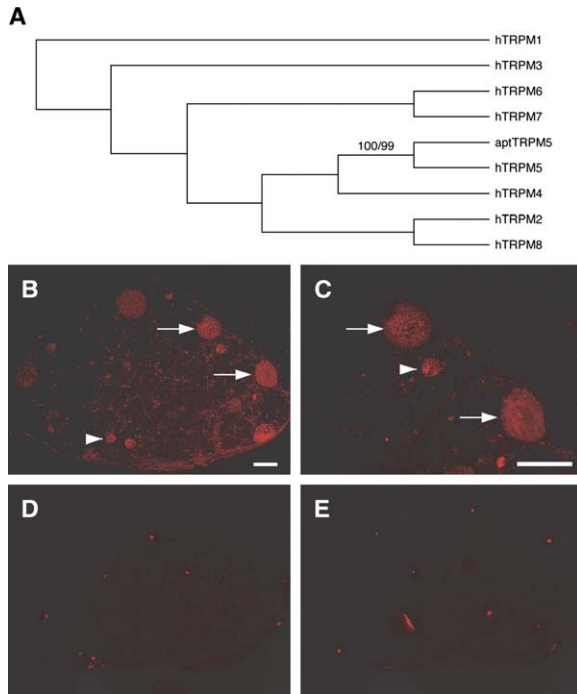


Figure 8. Pacemaker and Relay Neurons Express TRPM5
(A) Cladogram of the amino acid sequence of the cloned *Apterontus* TRPM5 and mammalian TRPM family. Sequences were aligned with Clustal X and analyzed with PAUP*. Neighbor-joining and parsimony methods (1000 bootstrap replicates each) strongly support aptTRPM5 as being an ortholog of the mammalian TRPM5 (Bootstrap values are 100 for NJ and 99 for pars.). (B and C) PMn sections hybridized with digoxigenin-labeled antisense aptTRPM5 RNA showed intense label in relay (arrows) and pacemaker (arrowheads) neurons. (D) PMn sections hybridized with labeled sense RNA or (E) labeled antisense RNA with excess unlabeled antisense RNA show no specific signal. Panels (B), (D), and (E) were taken at 20× magnification; panel (C) at 40× magnification. Scale bar, 100 μm.

personal communication) and TRP channels and are coupled via an extensive network of gap junctions, activation of either cell type leads to LTFE.

LTFE is induced, but not maintained, by synaptic input (Figure 6); a change in intrinsic excitability in the post-synaptic neurons in the PMn is the likely cause behind LTFE. Our pharmacological data suggest a type of non-specific cation channel, the TRP channel, as the final step of the LTFE signaling cascade (Figures 7B and 7C), and we have localized the TRPM5 subunit to the pacemaker and relay neurons of the pacemaker nucleus. Some members of this family, such as TRPM5, are directly activated by intracellular Ca^{2+} and therefore produce a Ca^{2+} -activated nonselective cation current (CAN) (Launay et al., 2002; Prawitt et al., 2003). CAN currents, which have been described in a number of other neuronal systems, inactivate slowly and therefore are capable of maintaining sustained depolarizations and, with that, increases in spike frequency (Partridge et al., 1994; Partridge and Valenzuela, 2000). Further, it has been reported that TRP-based CAN currents are involved in generating a synaptically driven, graded persistent increase in spike frequency in the entorhinal cortex (Egorov et al., 2002; B. Tahvildari et al., 2004, Soc. Neurosci., abstract). In the PMn, a long-lasting depolar-

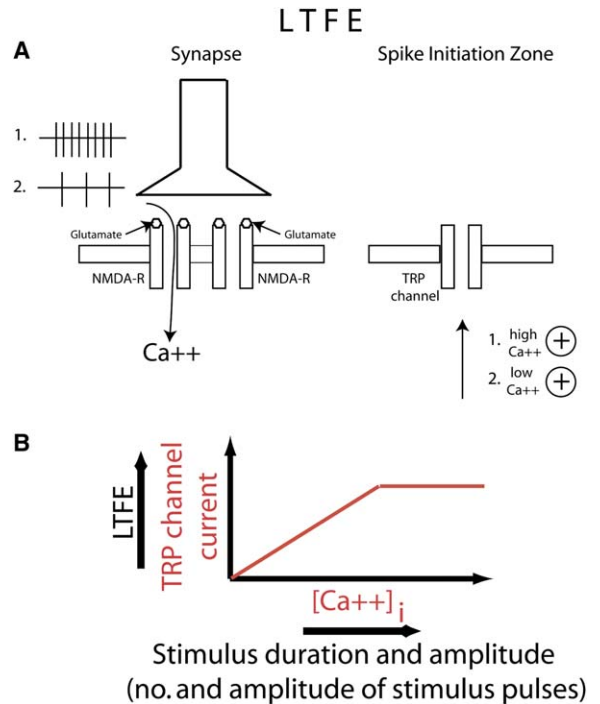


Figure 9. Model for the LTFE Mechanism
(A) LTFE is induced in the PMn by activation of NMDA-receptor carrying synapses from the afferent fibers of the prepacemaker nuclei (Dye et al., 1989; Heiligenberg et al., 1996; Juranek and Metzner, 1998). Stimulus duration and amplitude translate into number and amplitude of stimulus pulses (the latter presumably recruiting more afferent fibers). At low stimulus durations and/or amplitudes, less Ca^{2+} flows through NMDA receptors into the cell (1), whereas at higher durations and/or amplitudes, more Ca^{2+} enters the cell (2). (B) Low and high Ca^{2+} concentration activate the long-term enhancement of a TRP channel-based current in a linear fashion. The graded depolarization caused by the current underlies the long-term increase in PMn frequency (LTFE).

ization following closely the time course of LTFE can also be noted after tetanic stimulations (Dye, 1988). Therefore, a possible scenario for the mechanism behind graded LTFE in the electromotor PMn is that Ca^{2+} influx over NMDA receptors could directly or indirectly activate a CAN-like TRP channel (Baba et al., 2003; Chinopoulos et al., 2004; Zhu et al., 2005), which then maintains a sustained depolarization and with that an increase in spike frequency, linearly depending on the amount of Ca^{2+} flowing into the cell (Figure 9). Thus, the second stage is the long-term accumulation of activated TRP channels.

The presence of a seemingly similar mechanism in fish hindbrain and mammalian cortex (Egorov et al., 2002; B. Tahvildari et al., 2004, Soc. Neurosci., abstract) suggests that this could be a widespread mechanism for the formation of graded memories.

Experimental Procedures

Animals

Wild-caught individuals of *A. leptorhynchus* were obtained through different vendors and then housed in individual and community plexiglas tanks in climate-controlled rooms with a circulating water system and a dark-light cycle of 12/12 hr. The temperature in the rooms was held stable between approximately 26°C–28°C and the

water conditions were relatively constant. Fish were fed with frozen brine shrimp every 2 days.

PMn Slice Preparation

PMn slice preparation was performed as previously described (Oestreich and Zakon, 2002). In short, the ventral portion of the brainstem, spanning from a point in close proximity of the caudal aspect of the pacemaker nucleus to the pituitary fossa, was transferred to the recording well of a plexiglas tissue slice chamber, where it was continuously perfused with ACSF.

The tissue was maintained in a fluid interface and a humidified gas mixture from an outer water bath (flowrate = 8 l/min) constantly streamed over the tissue. Because of the high gas flow rate, the temperature of the slice chamber was uniform, and gas and saline temperature were adequately regulated by controlling the temperature in the outer water bath (temperature controller: TR-100, Fine Science Tools, North Vancouver, B.C., Canada) and kept constant at 24°C.

In experiments examining the role of Ca²⁺ and TRP channel antagonists, the PMns were submerged to facilitate washout of drugs.

PMn Recordings

The method was as outlined previously (Oestreich and Zakon, 2002). In short, recordings of the extracellular compound potential of the PMn were made with a homemade blunt tungsten wire electrode, amplified, A/D-converted, and digitally recorded. The PMn frequency was constantly monitored during the experiment. After the frequency reached stability, the tissue rostral to the PMn, which contains the afferent fiber pathways, was stimulated through a self-made bipolar silver wire electrode. The stimulus parameters were as followed: pulse width = 400 μ s (the same in all experiments), either three pulses spaced 25 ms apart, or in some cases one pulse every 250 ms. Train frequencies ranged from 0.5–6 Hz for the low-frequency stimulations. In case of the high-frequency stimulations without drug applications, pulses were delivered at 1000 Hz for 1 s. In experiments investigating the role of Ca²⁺ and TRP channel activation, two tetanic stimulus bouts of 500 Hz for 1 s each were applied. In all cases, bouts were spaced 2 min apart. Stimulus amplitude in some of the low-frequency experiments ranged from 10 to 100 nA; in high-frequency experiments it was 100 nA.

Pharmacology

(\pm)-CPP ((\pm)-3-(2-Carboxypiperazin-4-yl)propyl-1-phosphonic acid) was obtained from Sigma-Aldrich Co. (St. Louis, MO), and ω -Conotoxin GVIA from Sigma-Aldrich Co. and Alomone Labs Ltd. (Jerusalem, Israel). Both drugs were dissolved in deionized water to a concentration twice that used in the final experiments. The pH value of the CPP solution was adjusted to 7.2–7.4, comparable to the pH of the oxygenated ACSF. Aliquots of both drugs were stored at –20°C. Before the experiment, aliquots were thawed and sonicated briefly and then mixed with an equal volume of ACSF for a final concentration of 5–30 mM for CPP and 165 μ M for the conotoxin. Perfusion was stopped 20 min before stimulation to prevent drugs from washing out and to give the preparation enough time to acclimate to the new conditions. This sometimes resulted in a temporary increase in PMn frequency of a few Hertz, but did not noticeably affect the survival time of the PMn within the duration of the experiment. CPP (final concentration estimated as 60–80 μ M for 5 mM stock, 180–240 μ M for 15 mM stock, and 360–480 μ M for 30 mM stock according to Dye et al., 1989; all cited concentrations are the highest estimated concentration) was applied 5 min before stimulation, and the conotoxin (final concentration estimated as 2–3 μ M) 20 min before stimulation. 15 μ l of each drug were pressure-applied into the fluid interface covering the rostral aspect of the slice through a 5 M Ω patch pipette (Picospritzer II, General Valve Corporation, Fairfield, NJ), using 40 ms puffs at 3–5 Pa. BSA (0.5 mg/ml; Sigma-Aldrich) was added to the ACSF when using ω -conotoxin GVIA to prevent the toxin from binding to the plexiglas of the slice chamber by preblocking possible peptide binding sites (Luo et al., 1998; Tabata et al., 1996). In addition, the slice chamber was pretreated with a silicone solution (Sigmacote, Sigma-Aldrich) for the same reasons. Further, after each experiment, everything in the slice chamber that had come in contact with the conotoxin was cleansed by sonication for 30–60 min with an enzyme cleaner (Zymit, International Products Corp., Burlington, NJ).

We used a relatively high concentration of CPP (highest estimated final concentration of 360–480 μ M; Dye et al., 1989; CPP is reported to induce complete block from 1–100 μ M, depending on the composition of the NMDA receptor subunits expressed in *Xenopus* oocytes, Feng et al., 2005) in this experiment to ensure a complete block of the NMDA receptors and to overcome access problems. The PMn slice is >1 mm thick, with few neuronal somata surrounded by large numbers of heavily myelinated fibers in a dense and tight neuropil that appears to form a barrier to diffusion of hydrophilic compounds. This was a problem faced by previous investigators who also had to use comparably high concentrations of CPP and related drugs (Dye et al., 1989; Heiligenberg et al., 1996). We tested the specificity of CPP at this concentration by coapplying either NMDA or kainate (the PMn responds poorly to quisqualate [Dye et al., 1989] or AMPA [J.O., unpublished data], suggesting that its predominant class of non-NMDA receptors are kainate receptors) with CPP and found that CPP significantly reduced the NMDA-induced PMn frequency increase ($p < 0.05$), but did not block the kainate-induced frequency increase.

In experiments examining the role of TRP channel antagonists, drugs were bath applied. Flufenamic acid and SKF 96365 were made fresh daily. Both of these compounds were first dissolved in dimethylsulfoxide (DMSO) at 1000 \times the desired concentration and were subsequently diluted in ACSF such that DMSO was 0.1%. Other pharmacological reagents were made at 1000 \times in deionized H₂O and stored (–20°C) in aliquots for future use. To induce LTFF_{NMDA}, 150 μ M NMDA was applied through the bath for a period of 20 s. All reagents were acquired from Sigma-Aldrich.

Cloning and In Situ Hybridization of TRPM5

A 560 bp fragment of TRPM5 (GenBank accession number: bankit757517) was amplified from *Apteronotus leptorhynchus* brain mRNA using a series of nested RT-PCRs (One-Step RT-PCR, Invitrogen, Carlsbad, CA). Primers were designed to match highly conserved regions in the mouse, human, and rat TRPM5 and the predicted TRPM5 sequences deduced from the zebrafish (*Danio rerio*: http://www.ensembl.org/Danio_rerio/blastview) and pufferfish genomes (*Tetraodon nigrividius*: <http://www.genoscope.cns.fr/>) (dF2369 = 5'-GTC ATC ATG TAC TTT GCY TTC CTC; dR2919 = 5'-CAG CAT CTA TTT CCT CCA RRG GRA TC). RT-PCR products were cloned into TOPO pCR2.1 vector (Invitrogen, Carlsbad, CA) and sequenced using onsite facilities (dNA Tools, University of Texas at Austin, Austin, TX).

For in situ hybridization, fish were sacrificed, and brains were immediately snap-frozen in 2-methylbutane and were sectioned (20 μ m). RNA probes were generated with the MAXscript in vitro transcription system (Ambion, Austin, TX). Briefly, T3 and T7 promoter sequences were adapted to gene-specific forward and reverse primers for TRPM5 to amplify templates. PCR products were size-resolved by gel electrophoresis and, after template purification, RNAs, ~400 nucleotides in length, were transcribed incorporating digoxigenin-labeled UTPs in either sense or antisense orientations. In addition, antisense RNA was transcribed without digoxigenin-labeled UTPs, as an internal control, to compete against labeled RNA during hybridization.

Sections were fixed in 4% paraformaldehyde and incubated with proteinase K (0.1 μ g/ml) in 0.1 M Tris and 0.05 M EDTA (pH 8.0) for 10 min at 25°C. Sections were then acetylated, delipidated with chloroform, and serially dehydrated with ethanol. Sections were incubated in prehybridization solution containing final concentrations of tRNA (250 μ g/ml), 25% formamide, 10% dextran sulfate, 2.5 \times Denhardt's solution, 0.05 mg/ml salmon sperm DNA, 4 \times SSCP, 4 mM EDTA (pH 8.0) for 2 hr at 62°C. Sections were then incubated in hybridization solution containing antisense or sense probes (0.7 ng/ μ l) for 18 hr at 62°C.

After hybridization, sections were rinsed in a dilution series (2 \times to 0.1 \times) of SSC (at 45°C) and then immersed in 1 \times PBS for 5 min and incubated 1 hr (25°C) in 1 \times PBS with 1% BSA containing Rhodamine Red-X anti-digoxigenin antibody conjugates (Invitrogen, Carlsbad, CA, 1:200). Sections were subsequently rinsed three times in PBS with 0.25% BSA (15 min each wash), coverslipped, and subjected to fluorescence microscopy and image analysis using Image Pro Plus v. 4.1 (Media Cybernetics, Inc, Silver Spring, MD).

Statistical Analysis

All statistical analysis was performed using Graphpad Prism 4.01 (Graphpad Software Inc., San Diego CA), with the exception of the conotoxin experiments. Here, means were compared using Microsoft Excel's build-in "TTest" worksheet function to determine significance (calculates p value for unpaired, two-tailed Student's t test; Excel 2000, Microsoft Corp., Redmond, WA). p values reported in the text are averages for the parts of the curve before, during, and after the stimulation. In general, values are reported as mean \pm standard error of the mean. Multiple pairwise comparisons were performed by ANOVA, followed by Newman-Keuls post hoc analysis, unless noted differently in the text. All t tests performed for single pairwise comparisons were unpaired, two-tailed Student's t tests. Slopes of linear regression lines were compared by using Graphpad's build-in function, which is based on an ANCOVA.

Acknowledgments

The authors would like to acknowledge Maggie Patay for fish care; Marianna Grenadier for artwork; and He Liu for guidance in molecular biology. This work was funded by NIMH R01 MH56535 and F32 NS046949.

Received: July 25, 2005

Revised: December 5, 2005

Accepted: January 29, 2006

Published: February 15, 2006

References

- Baba, A., Yasui, T., Fujisawa, S., Yamada, R.X., Yamada, M.K., Nishiyama, N., Matsuki, N., and Ikegaya, Y. (2003). Activity-evoked capacitative Ca²⁺ entry: implications in synaptic plasticity. *J. Neurosci.* **23**, 7737–7741.
- Bottai, D., Dunn, R.J., Ellis, W., and Maler, L. (1997). N-methyl-D-aspartate receptor 1 mRNA distribution in the central nervous system of the weakly electric fish *Apteronotus leptorhynchus*. *J. Comp. Neurol.* **389**, 65–80.
- Bottai, D., Maler, L., and Dunn, R.J. (1998). Alternative RNA splicing of the NMDA receptor NR1 mRNA in the neurons of the teleost electrosensory system. *J. Neurosci.* **18**, 5191–5202.
- Bullock, T.H., Hamstra, R.H., and Scheich, H. (1972). The jamming avoidance response of high frequency electric fish. II. Quantitative aspects. *J. Comp. Physiol.* **77**, 23–48.
- Chinopoulos, C., Gerencser, A.A., Doczi, J., Fiskum, G., and Adam-Vizi, V. (2004). Inhibition of glutamate-induced delayed calcium deregulation by 2-APB and La³⁺ in cultured cortical neurones. *J. Neurochem.* **91**, 471–483.
- Daw, N.W., Stein, P.S., and Fox, K. (1993). The role of NMDA receptors in information processing. *Annu. Rev. Neurosci.* **16**, 207–222.
- Dulka, J.G., and Maler, L. (1994). Testosterone modulates female chirping behavior in the weakly electric fish, *Apteronotus leptorhynchus*. *J. Comp. Physiol. [A]* **174**, 331–343.
- Dye, J. (1987). Dynamics and stimulus-dependence of pacemaker control during behavioral modulations in the weakly electric fish, *Apteronotus*. *J. Comp. Physiol. [A]* **161**, 175–185.
- Dye, J. (1988). An in vitro physiological preparation of a vertebrate communicatory behavior: chirping in the weakly electric fish, *Apteronotus*. *J. Comp. Physiol. [A]* **163**, 445–458.
- Dye, J., and Heiligenberg, W. (1987). Intracellular recording in the medullary pacemaker nucleus of the weakly electric fish, *Apteronotus*, during modulatory behaviors. *J. Comp. Physiol. [A]* **161**, 187–200.
- Dye, J., Heiligenberg, W., Keller, C.H., and Kawasaki, M. (1989). Different classes of glutamate receptors mediate distinct behaviors in a single brainstem nucleus. *Proc. Natl. Acad. Sci. USA* **86**, 8993–8997.
- Eder, C., Klee, R., and Heinemann, U. (1998). Involvement of stretch-activated Cl⁻ channels in ramification of murine microglia. *J. Neurosci.* **18**, 7127–7137.
- Egorov, A.V., Hamam, B.N., Franssen, E., Hasselmo, M.E., and Alonso, A.A. (2002). Graded persistent activity in entorhinal cortex neurons. *Nature* **420**, 173–178.
- Feng, B., Morley, R.M., Jane, D.E., and Monaghan, D.T. (2005). The effect of competitive antagonist chain length on NMDA receptor subunit selectivity. *Neuropharmacology* **48**, 354–359.
- Hagedorn, M., and Heiligenberg, W. (1985). Court and spark: electric signals in the courtship and mating of gymnotoid fish. *Anim. Behav.* **33**, 254–265.
- Harks, E.G., de Roos, A.D., Peters, P.H., de Haan, L.H., Brouwer, A., Ypey, D.L., van Zoelen, E.J., and Theuvsen, A.P. (2001). Fenamates: a novel class of reversible gap junction blockers. *J. Pharmacol. Exp. Ther.* **298**, 1033–1041.
- Harvey-Girard, E., and Dunn, R.J. (2003). Excitatory amino acid receptors of the electrosensory system: the NR1/NR2B N-methyl-D-aspartate receptor. *J. Neurophysiol.* **89**, 822–832.
- Heiligenberg, W. (1991). *Neural Nets in Electric Fish* (Cambridge, MA: MIT Press).
- Heiligenberg, W., Metzner, W., Wong, C.J., and Keller, C.H. (1996). Motor control of the jamming avoidance response of *Apteronotus leptorhynchus*: evolutionary changes of a behavior and its neuronal substrates. *J. Comp. Physiol. [A]* **179**, 653–674.
- Held, R., and Freedman, S.J. (1963). Plasticity in human sensorimotor control. *Science* **142**, 455–462.
- Hill, K., Benham, C.D., McNulty, S., and Randall, A.D. (2004). Flufenamic acid is a pH-dependent antagonist of TRPM2 channels. *Neuropharmacology* **47**, 450–460.
- Hofmann, T., Chubanov, V., Gudermann, T., and Montell, C. (2003). TRPM5 is a voltage-modulated and Ca²⁺-activated monovalent selective cation channel. *Curr. Biol.* **13**, 1153–1158.
- Inoue, R., Okada, T., Onoue, H., Hara, Y., Shimizu, S., Naitoh, S., Ito, Y., and Mori, Y. (2001). The transient receptor potential protein homologue TRP6 is the essential component of vascular alpha(1)-adrenoceptor-activated Ca²⁺-permeable cation channel. *Circ. Res.* **88**, 325–332.
- Juranek, J., and Metzner, W. (1998). Segregation of behavior-specific synaptic inputs to a vertebrate neuronal oscillator. *J. Neurosci.* **18**, 9010–9019.
- Launay, P., Fleig, A., Perraud, A.L., Scharenberg, A.M., Penner, R., and Kinet, J.P. (2002). TRPM4 is a Ca²⁺-activated nonselective cation channel mediating cell membrane depolarization. *Cell* **109**, 397–407.
- Lee, Y.M., Kim, B.J., Kim, H.J., Yang, D.K., Zhu, M.H., Lee, K.P., So, I., and Kim, K.W. (2003). TRPC5 as a candidate for the nonselective cation channel activated by muscarinic stimulation in murine stomach. *Am. J. Physiol. Gastrointest. Liver Physiol.* **284**, G604–G616.
- Luo, S., Kulak, J.M., Cartier, G.E., Jacobsen, R.B., Yoshikami, D., Olivera, B.M., and McIntosh, J.M. (1998). alpha-conotoxin AulB selectively blocks alpha3 beta4 nicotinic acetylcholine receptors and nicotine-evoked norepinephrine release. *J. Neurosci.* **18**, 8571–8579.
- Meir, A., Ginsburg, S., Butkevich, A., Kachalsky, S.G., Kaiserman, I., Ahdut, R., Demigoren, S., and Rahamimoff, R. (1999). Ion channels in presynaptic nerve terminals and control of transmitter release. *Physiol. Rev.* **79**, 1019–1088.
- Moortgat, K.T., Bullock, T.H., and Sejnowski, T.J. (2000a). Gap junction effects on precision and frequency of a model pacemaker network. *J. Neurophysiol.* **83**, 984–997.
- Moortgat, K.T., Bullock, T.H., and Sejnowski, T.J. (2000b). Precision of the pacemaker nucleus in a weakly electric fish: network versus cellular influences. *J. Neurophysiol.* **83**, 971–983.
- Oestreich, J., and Zakon, H.H. (2002). The long-term resetting of a brainstem pacemaker nucleus by synaptic input: a model for sensorimotor adaptation. *J. Neurosci.* **22**, 8287–8296.
- Oestreich, J., and Zakon, H.H. (2005). Species-specific differences in sensorimotor adaptation are correlated with differences in social structure. *J. Comp. Physiol. A Neuroethol. Sens. Neural Behav. Physiol.* **191**, 845–856.
- Partridge, L.D., and Valenzuela, C.F. (2000). Block of hippocampal CAN channels by flufenamate. *Brain Res.* **867**, 143–148.

- Partridge, L.D., Muller, T.H., and Swandulla, D. (1994). Calcium-activated non-selective channels in the nervous system. *Brain Res. Brain Res. Rev.* *19*, 319–325.
- Prawitt, D., Monteilh-Zoller, M.K., Brixel, L., Spangenberg, C., Zabel, B., Fleig, A., and Penner, R. (2003). TRPM5 is a transient Ca²⁺-activated cation channel responding to rapid changes in [Ca²⁺]_i. *Proc. Natl. Acad. Sci. USA* *100*, 15166–15171.
- Smith, G.T., and Zakon, H.H. (2000). Pharmacological characterization of ionic currents that regulate the pacemaker rhythm in a weakly electric fish. *J. Neurobiol.* *42*, 270–286.
- Smith, G.T., Lu, Y., and Zakon, H.H. (2000). Parvocells: a novel interneuron type in the pacemaker nucleus of a weakly electric fish. *J. Comp. Neurol.* *423*, 427–439.
- Spiro, J.E., Brose, N., Heinemann, S.F., and Heiligenberg, W. (1994). Immunolocalization of NMDA receptors in the central nervous system of weakly electric fish: functional implications for the modulation of a neuronal oscillator. *J. Neurosci.* *14*, 6289–6299.
- Srinivas, M., and Spray, D.C. (2003). Closure of gap junction channels by arylaminobenzoates. *Mol. Pharmacol.* *63*, 1389–1397.
- Tabata, T., Olivera, B.M., and Ishida, A.T. (1996). Omega-conotoxin-MVIIID blocks an omega-conotoxin-GVIA-sensitive, high-threshold Ca²⁺ current in fish retinal ganglion cells. *Neuropharmacology* *35*, 633–636.
- Tallarovic, S.K., and Zakon, H.H. (2002). Electrocommunication signals in female brown ghost electric knifefish, *Apteronotus leptorhynchus*. *J. Comp. Physiol. [A]* *188*, 649–657.
- Tesfai, Y., Brereton, H.M., and Barritt, G.J. (2001). A diacylglycerol-activated Ca²⁺ channel in PC12 cells (an adrenal chromaffin cell line) correlates with expression of the TRP-6 (transient receptor potential) protein. *Biochem. J.* *358*, 717–726.
- Tozzi, A., Bengtson, C.P., Longone, P., Carignani, C., Fusco, F.R., Bernardi, G., and Mercuri, N.B. (2003). Involvement of transient receptor potential-like channels in responses to mGluR-I activation in midbrain dopamine neurons. *Eur. J. Neurosci.* *18*, 2133–2145.
- Ullrich, N.D., Voets, T., Prenen, J., Vennekens, R., Talavera, K., Droogmans, G., and Nilius, B. (2005). Comparison of functional properties of the Ca²⁺-activated cation channels TRPM4 and TRPM5 from mice. *Cell Calcium* *37*, 267–278.
- van Rossum, D.B., Patterson, R.L., Ma, H.T., and Gill, D.L. (2000). Ca²⁺ entry mediated by store depletion, S-nitrosylation, and TRP3 channels. Comparison of coupling and function. *J. Biol. Chem.* *275*, 28562–28568.
- Zhu, X., Jiang, M., and Birnbaumer, L. (1998). Receptor-activated Ca²⁺ influx via human Trp3 stably expressed in human embryonic kidney (HEK)293 cells. Evidence for a non-capacitative Ca²⁺ entry. *J. Biol. Chem.* *273*, 133–142.
- Zhu, Z.T., Munhall, A., Shen, K.Z., and Johnson, S.W. (2005). NMDA enhances a depolarization-activated inward current in subthalamic neurons. *Neuropharmacology* *49*, 317–327.